JOURNAL OF THE AMERICAN CHEMICAL SOCIETY

Article

para-Selective alkylation of benzamides and aromatic ketones by cooperative nickel/aluminum catalysis

Shogo Okumura, Shu-Wei Tang, Teruhiko Saito, Kazuhiko Semba, Shigeyoshi Sakaki, and Yoshiaki Nakao

J. Am. Chem. Soc., **Just Accepted Manuscript** • DOI: 10.1021/jacs.6b08767 • Publication Date (Web): 19 Oct 2016

para-Selective Alkylation of Benzamides and Aromatic Ketones by Cooperative Nickel/Aluminum Catalysis

Shogo Okumura,[†] Shuwei Tang,[‡] Teruhiko Saito,[†] Kazuhiko Semba,[†] Shigeyoshi Sakaki,[‡,*] and Yoshiaki Nakao[†,*]

[†]Department of Material Chemistry, Graduate School of Engineering, Kyoto University, Kyoto 615-8510, Japan and [‡]Fukui Institute for Fundamental Chemistry, Kyoto University, Sakyo-ku, Kyoto 606-8103, Japan

ABSTRACT: We report a method that ensures the selective alkylation of benzamides and aromatic ketones at the *para*-position *via* cooperative nickel/aluminum catalysis. Using a bulky catalyst/co-catalyst system allows reactions between benzamides with alkenes to afford the corresponding *para*-alkylated products. The origin of the high *para*-selectivity has also been investigated by density functional theory calculations.

The introduction of alkyl groups on a benzene ring is a fundamentally important transformation. Among various possible ways to alkylate the aromatic core, the alkylation reaction using alkenes serves as an ideal transformation in terms of atom-economy[1] as well as the availability of alkene feedstock in the chemical industry. For example, around 70% of benzene is supplied for the alkylation reaction with ethylene and propylene to produce ethylbenzene and cumene, which are further converted to styrene and phenol/acetone, respectively, on industrial scales.[2] The alkylation of substituted benzenes, in particular electron-poor ones such as aromatic carbonyl compounds, still suffers from systematic drawbacks. The electron-withdrawing carbonyl groups limit the scope of alkyl groups that can be introduced at the *meta*-position by acid-catalyzed aromatic electrophilic substitutions using reactive alkylating agents such as alkyl ethers.[3] Recent advances in metal-catalyzed direct C–H alkylation[4] have made the introduction of both linear[5] and branched[6] alkyl groups at the *ortho*-position possible (Eq. 1), predominantly via the coordination of the carbonyl group to a metal catalyst. Conversely, to the best of our knowledge, the only examples that provide an effective *para*-selective alkylation of electron-deficient arenes involve the introduction of a limited number of cyclic alkyl groups *via* nucleophilic substitution with radical species generated from cycloalkanes as reaction solvents in the presence of a ruthenium catalyst and di-*tert*-butyl peroxide.[7] Here, we demonstrate an effective direct *para*-alkylation of benzamides and aromatic ketones with alkenes by cooperative nickel/Lewis acid (LA) catalysis (Eq. 2). We chose this catalytic system with the expectation that the coordination of the carbonyl groups to the LA would enhance the reactivity of the electron-deficient arenes towards the electron-rich nickel(0) catalyst. Moreover, we speculated that the steric repulsion between the nickel catalyst and the LA should increase the *para*-selectivity relative to reactions at *ortho*- and *meta*-positions. Progress in *para*-selective direct arene C–H functionalizations still remain limited; reported examples are either restricted to electron-rich arenes,[8–14] to specific arenes with bulky substituents[15,16] or to substrates with a directing group.[17]

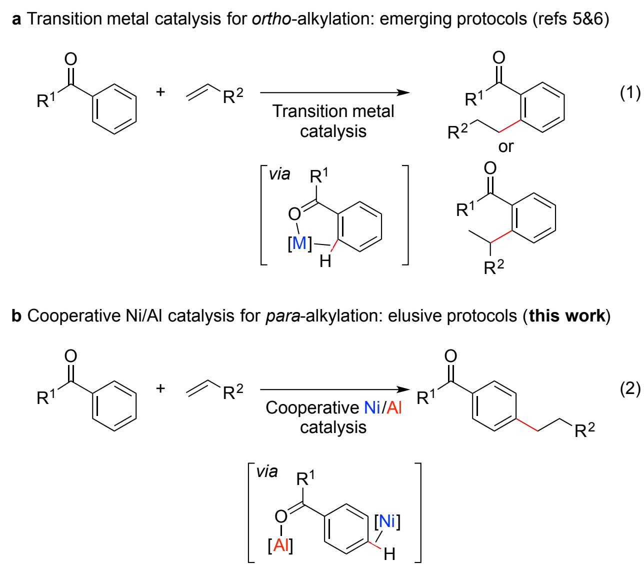

We have previously reported that the direct alkylation of pyridine derivatives with alkenes proceeds selectively at the C-4 position of the pyridine moiety by cooperative catalysis using bis(1,5-cyclooctadiene)nickel [Ni(cod)$_2$], *N*-heterocyclic carbene (NHC) as a ligand for nickel, and the bulky LA co-catalyst (2,6-*t*-Bu$_2$–4-Me–C$_6$H$_2$O)$_2$AlMe (MAD).[18] As a starting point for this investigation, we used the same catalyst system using **L1** [1,3-bis(2,6-diisopropylphenyl)imidazo-2-ylidene] as a ligand for the reaction between *N*,*N*-diethylbenzamide (**1a**) and 1-tridecene (**2a**). However, the corresponding *para*- and *meta*-alkylbenzamides (**3aa** and **3'aa**) were obtained only in low yield (4%) and moderate regioselectivity (**3aa**/**3'aa** = 61:39; entry 1, Table 1). We then decided to screen both potential ligands and LAs, and

Table 1. Conditions for the Alkylation of *N*,*N*-Diethylbenzamide (**1a**) with 1-Tridecene (**2a**)

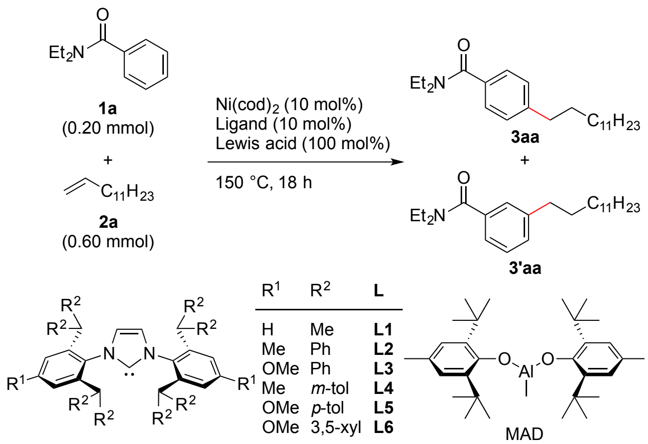

entry	ligand	Lewis acid	yield (%)[a]	3aa/3'aa [a]
1	**L1**	MAD	4	61:39
2	**L2**	MAD	40	66:34
3	**L3**	MAD	60	64:36
4	**L4**	MAD	4	81:19
5	**L5**	MAD	44	60:40
6	**L6**	MAD	86	93:7
7	**L6**	$AlMe_3$	34	81:19
8	**L6**	none	7	58:42

[a] Determined by gas chromatography analysis using *n*-dodecane as an internal standard and not corrected for response factors of minor isomers.

found that the use of bulky NHC ligands such as **L2**[19] increased the yield to 40% (entry 2, Table 1), and that the use of the equally bulky and more electron-donating NHC ligand **L3**[20] furnished a yield of up to 60% (entry 3, Table 1). However, for both ligands, no improvement regarding the selectivity was observed. We therefore turned our attention to the tuning of steric effects via the modulation of the terminal phenyl groups in **L2** or **L3**. A significant increase in regioselectivity (**3aa**/**3'aa** = 81:19) was observed for **L4** carrying *m*-tolyl groups (entry 4, Table 1), whereas *p*-tolyl groups in **L5** did not affect the **3aa**/**3'aa** ratio (entry 5, Table 1). Ultimately, the best performance was observed for **L6** with 3,5-xylyl groups, which resulted in a *para*-selective (**3aa**/**3'aa** = 93:7) alkylation in 86% combined yield (entry 6, Table 1). The use of sterically undemanding $AlMe_3$ as a co-catalyst proved to be detrimental for the reaction yield (entry 7, Table 1), while the absence of an aluminum-based LA resulted in both poor yield and regioselectivity (entry 8, Table 1). Combined, these observations indicate that the steric factors associated with ligand and co-catalyst most likely play a key role in the control of the regioselectivity.

Using the $Ni(cod)_2$/**L6** system in combination with the co-catalyst MAD, we carried out the alkylation of **1a** with a variety of alkenes (Table 2). For example, using **2a** on a preparative scale (1.0 mmol) afforded a mixture of *para*- and *meta*-alkylation products (**3aa**/**3'aa** = 92:8) in 67% yield. Allyl(triethoxy)silane (**2b**) also reacted with **1a** to give the corresponding *para*-alkylation product, which was further subjected to the Tamao–Fleming oxidation[21] to give **3ab**. 1-Alkenes that contain bulky substituents such as vinylcyclohexane (**2c**), 3,3-dimethyl-1-butene (**2d**), 5-(*tert*-butyldimethylsilyloxy)-3,3-dimethyl-1-pentene (**2e**), trimethyl(vinyl)silane (**2f**), and

Table 2. Substrate Scope for the *para*-Selective Alkylation of Benzamides

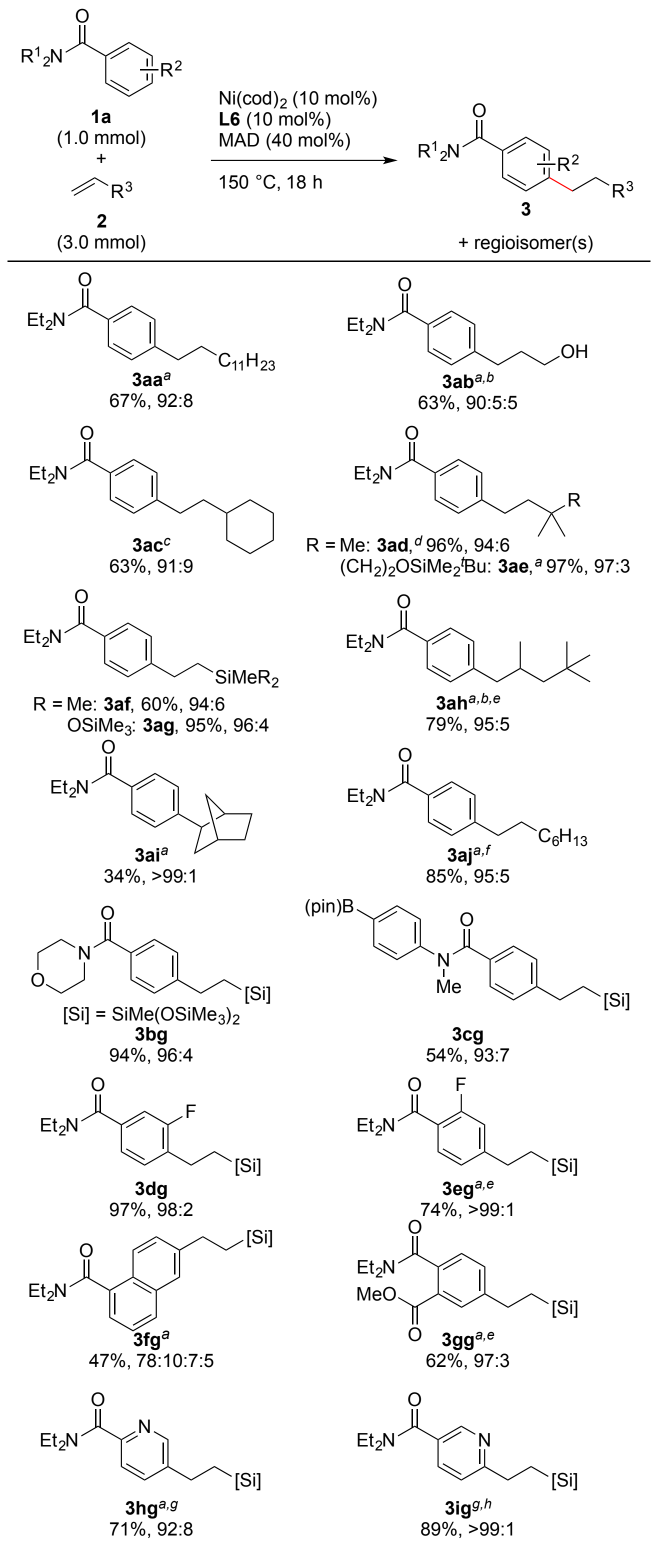

Yields were determined from the combined mass of the purified product mixtures. The product ratios were determined by GC analysis of the crudes. [a] Run with 100 mol% MAD. [b] Run with allyl(triethoxy)silane followed by the Tamao–Fleming oxidation. [c] Run with 5.0 mmol **2**. [d] Run with 7.0 mmol **2d**. [e] Run with 20 mol% $Ni(cod)_2$/**L6**. [f] Run with 5.0 mmol **2j**. [g] Run with toluene (1.0 mL) as a solvent at 135 °C. [h] Run for 7.5 h.

methylbis(trimethylsilyloxy)vinylsilane (**2g**) all reacted with **1a** to yield the corresponding *para*-alkylated benzamides (**3ac**–**3ag**). Notably, with some of these bulky alkene substrates, MAD can be used in catalytic amounts. The multi-substituted double bonds of 2,4,4-trimethyl-1-pentene (**2h**) and norbornene (**2i**) also engaged in the *para*-selective alkylation of **1a** (**3ah** and **3ai**), whereas the internal double bond of 2-octene (**2j**) was isomerized to the terminal position prior to affording the linear *para*-alkylation product (**3aj**). Unfortunately, styrene, cyclohexene, vinylboronate, and alkyl vinyl ether derivatives did not engage in such alkylation reactions (Table S1 of Supporting Information). Subsequently, we surveyed the scope of benzamides using vinylsilane **2g**, as this should provide products with convertible silyl groups.[22] Morpholino(phenyl)methanone (**1b**), whose aminocarbonyl functionality can be readily transformed to ketones by nucleophilic carbonyl substitution reactions,[23] afforded **3bg** in excellent yield and *para*-selectivity. Benzamide bearing an arylboronate functionality (**1c**) also participated in the alkylation at the position *para* to the aminocarbonyl group to give **3cg**. It is worth noting that a fluorine substituent at the *meta*- or *ortho*-position of **1a** (**1d** and **1e**, respectively) did not affect the *para*-alkylation reaction, even though it has been shown to perturb the selectivity of metal-catalyzed directed *ortho*-C–H alkylations.[24,25] A modest, yet clear C6-selectivity was observed for the alkylation of *N*,*N*-diethyl-1-naphthamide (**1f**). Moreover, the selective C–C bond formation at the position *para* to the aminocarbonyl group can be achieved in the presene of another carbonyl group of ester **1g** and *sp*^{2}-hybridized nitrogen of substituted pyridines **1h** and **1i**. The latter observation is particularly worth noting as we previously demonstrated that pyridines are alkylated at the C-4 position under similar reaction conditions.[18] This may be partly derived from the lowered Lewis basicity of the *sp*^{2}-nitrogen in **1h** and **1i** due to the presence of an electron-withdrawing aminocarbonyl group, because competitive reactions of **1h** or **1i** and pyridine with **2g** resulted preferentially in the C4-alkylation of pyridine (see Supporting Information).

Aromatic ketones were also alkylated in excellent *para*-selectivity (Table 3), whereas benzoates did not participate in the *para*-alkylation reaction under these reaction conditions (Table S2 of Supporting Information). The reaction of 4-dimethylaminobenzophenone (**4a**) with 1-octene (**2k**) and vinylcyclohexane (**2c**) proceeded in the presence of 20 mol% Ni/**L6** and 100 mol% MAD to give the corresponding alkylated arenes in 45% and 63% yield, respectively. As with the case of alkylation of benzamides, sterically demanding alkenes **2d**, **2f**, and **2g** reacted smoothly in the presence of a catalytic amount of MAD. Subsequently, we examined the scope of aromatic ketones using **2g** as an olefin coupling partner. The reaction of 4-methylbenzophenone (**4b**) in the presence of 40 mol% MAD at 150 °C for 18 h suffered from the formation of side products, which were likely derived form nucleophilic addition of the methyl group of MAD to the carbonyl moiety of **4b**. We thus performed the reaction in the presence of 10 mol% MAD at 100 °C to obtain the *para*-alkylation product in 52% yield with 99:1 regioselectivity and negligible amounts of the byproducts. Benzophenones bearing 4-phenyl (**4c**) and 4-siloxy (**4d**) groups gave the corresponding alkylated ketones with high *para*-selectivity. Alkyl aryl ketones such as ethyl phenyl ketone (**4e**), *tert*-butyl phenyl ketone (**4f**), and α-substituted indanone (**4g**) gave respective alkylated arenes with excellent *para*-selectivity. The use of 1 mol% MAD allowed the *para*-selective alkylation of 3-fluoroacetophenone (**4h**), which was contaminated by the Aldol condensation under the standard conditions with a higher loading of MAD.

Table 3. Substrate Scope for the *para*-Selective Alkylation of Aromatic Ketones

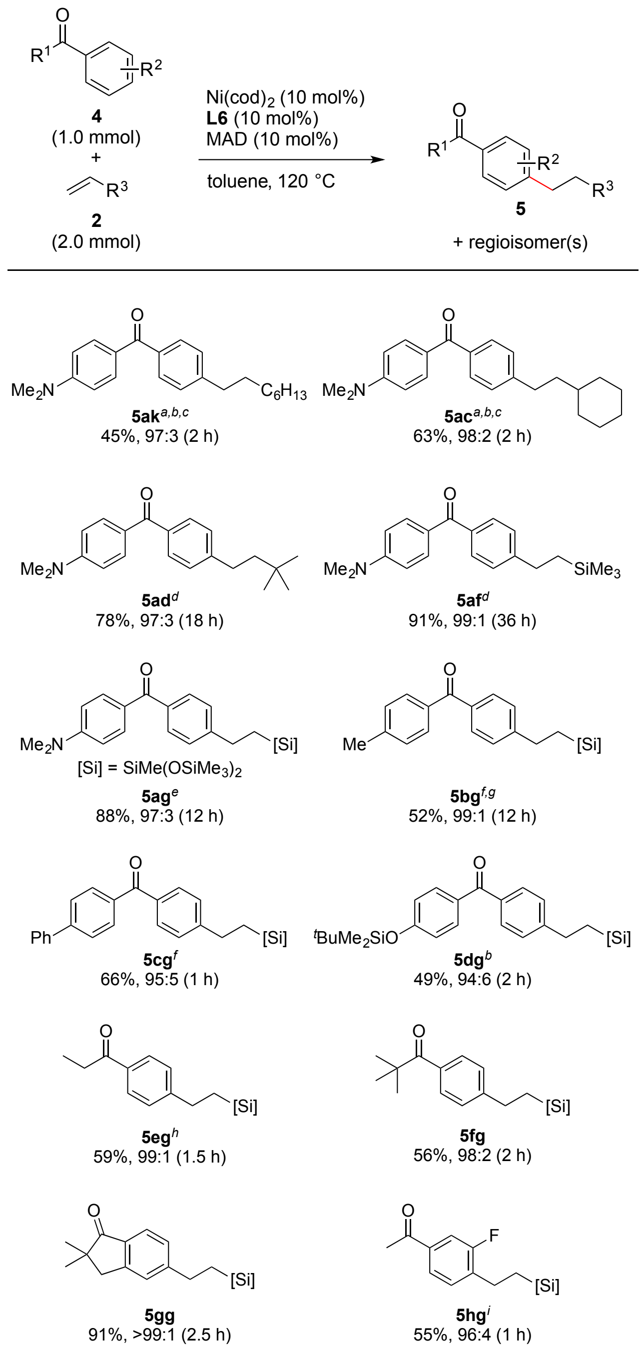

Yields were determined from the combined mass of the purified product mixtures. The product ratios were determined by GC analysis of the crudes. [a] Run with 20 mol% $Ni(cod)_2$/**L6**. [b] Run with 100 mol% MAD. [c] Run at 150 °C. [d] Run with 40 mol% MAD. [e] Run with 20 mol% MAD. [f] Run with 3.0 mmol **2**. [g] Run at 100 °C. [h] Run with 5 mol% $Ni(cod)_2$/**L6** [i] Run with 1 mol% MAD.

In order to gain an understanding of the reaction mechanism, alkylation reactions using **1a** and **1a**-d_5 were examined in parallel. The initial reaction rates were measured by gas chromatography analysis and afforded a value of 3.7 for the kinetic isotope effect (Figure S1 of Supporting Information). The reaction between **1a**-d_5 and **2g** for 3.5 h resulted in the loss of deuterium exclusively at the *para*-position of **1a**-d_5 and in partial deuteration of **2g** at the α-position (Eq. 3). These observations implied rate-limiting and reversible C–H activation exclusively at the *para*-position. Density functional theory (DFT) calculations were then carried out on the alkylation reaction of *N*,*N*-dimethylbenzamide with propene by (**L6**)Ni and $AlMe_3$, in order to develop a plausible catalytic cycle. The obtained energy profile is displayed in Figure 1a with geometrical changes (detailed changes are shown in Figure S2 and S3 of Supporting Information). Herein, bis(alkene)nickel complex **6** represents most likely a resting state of the catalytic cycle, because this is the most stable in possible reactant complexes. This species undergoes a ligand exchange reaction with *N*,*N*-dimethylbenzamide coordinating to $AlMe_3$, leading to the formation of σ-complex **9** *via* mono-alkene complexes **7** and **8**. Cleavage of the coordinated C–H bond and formation of one C–H and two C–Ni bonds should then proceed in a concerted manner in one step to furnish an alkyl(aryl)nickel complex **10**, in which an agostic interaction between H and Ni is observed. Then, geometric isomerization affords T-shaped alkyl(aryl)nickel intermediate **12** *via* its isomer **11**, and reductive elimination under concomitant formation of a C–C bond affords the alkylated arene–Ni complex **13**. The proposed catalytic cycle is consistent with a related mechanism for the nickel-catalyzed alkylation of 1,3-bis(trifluoromethyl)benzene, which was recently reported by Hartwig, Eisenstein, and coworkers.[26] In our theoretical study, the C–H activation step exhibits the highest activation barrier and should thus be considered as the rate-determining step of the catalytic cycle, which is supported by the observed kinetic isotope effect. The theoretical and experimental results show that the *para*-selectivity should thus be determined at the transition state $\mathbf{TS_{9-10}}$. The present DFT calculations successfully show the *para*-selectivity, which is enhanced by the presence of $AlMe_3$; 66:34 without $AlMe_3$ vs. *para*/*meta* = 98:2 with $AlMe_3$. The origin of the high *para*-selectivity in the presence of the aluminum Lewis acid cocatalyst can be explained in terms of electronic and steric factors, as will be discussed below.

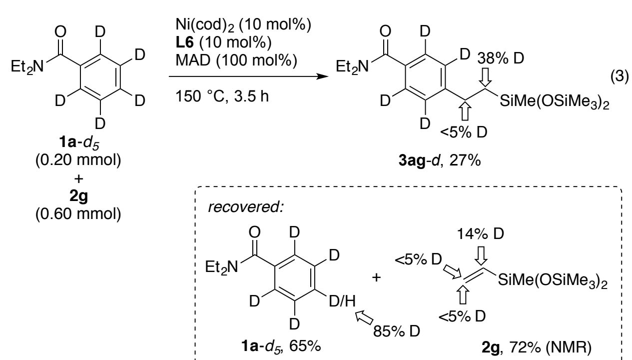

The activation energies are 35.4 and 37.3 kcal/mol for the *para*- and *meta*-alkylation in the absence of $AlMe_3$ (Figure 1b) but they are 30.8 and 33.2 kcal/mol in the presence of $AlMe_3$ (Figure 1a). These results clearly show that $AlMe_3$ accelerates the reaction. Qualitatively, *N*,*N*-dimethylbenzamide coordinating to $AlMe_3$ should show higher reactivity towards an electron-rich nickel(0) center at the *para*-position rather than at the *meta*-position. This notion was corroborated by the ^{1}H NMR analysis of the adduct **1a**–$AlMe_3$, which showed significant shifts for the signals associated with the *para*-hydrogen to lower field relative to those at the *meta*-position (see Supporting Information). The acceleration by $AlMe_3$ can be explained by the LUMO energy; the LUMO energy (–2.58 eV) of *N*,*N*-dimethylbenzamide coordinating to $AlMe_3$ is at lower energy than that of *N*,*N*-dimethylbenzamide (–2.05 eV) as shown in Figure 2. Because the LUMO consists of the σ* MO of the aromatic ring and the C–H σ* antibonding MO, the stronger CT to this LUMO leads to the easier C–H σ-bond cleavage. Indeed, the electron population of the *N*,*N*-dimethylbenzamide–$AlMe_3$ moiety increases more than that of *N*,*N*-dimethylbenzamide without $AlMe_3$, in the reaction from **7** to **10** (see Figure S5 of Supporting Information). Accordingly, it can be concluded that the aluminum Lewis acid accelerates the C–H σ-bond cleavage particularly at the *para*-position.

The *para*-selectivity also arises from a steric repulsion between the *m*-tolyl substituent of **L6** and the aluminum Lewis acid in $\mathbf{TS_{9-10}}$, which is larger in the case of the *meta*-C–H functionalization. The coordination of $AlMe_3$ group completely changes the orientation of the aminocarbonyl group of *N*,*N*-dimethylbenzamide to avoid the steric repulsion with the ligand substituents (Figure 3a vs Figure 3b). The extent of the congested geometry is larger in the transition state of *meta*-alkylation (Figure 3c) than in that of the *para*-alkylation (Figure 3b) in the presence of $AlMe_3$; the distances between the methyl groups of $AlMe_3$ (Cα and Cβ) and that of **L6** (C12) are much shorter in the former than in the latter. The steric factor should be more pronounced in the real catalytic system containing bulkier MAD, and the *para*-selectivity should be increased accordingly (entry 6 vs entry 7, Table 1), though the values calculated for **L6** and $AlMe_3$ show merely small differences for the respective activation barriers. Ligands lacking the methyl substituents in the *m*-tolyl group of **L6** (C12), such as **L1**–**L3** and **L5**, thus show poor *para*-selectivity because they do not induce this steric repulsion (entries 1–3 and entry 5 of Table 1). The absence of the aluminum Lewis acid cocatalyst gives the worst selectivity and poor reactivity even with **L6** as a ligand due to the lack of both the electronic activation and the steric repulsion (entry 8, Table 1).

In summary, we have demonstrated that the challenging *para*-selective alkylation of benzamides and aromatic ketones can be accomplished effectively by a cooperative catalysis based on a bulky NHC-ligated nickel catalyst and a bulky aluminum co-catalyst. The experimentally obtained results are fully supported by the results of theoretical calculations on appropriate model compounds, and a plausible reaction mechanism including the origin of the high *para*-selectivity is proposed.

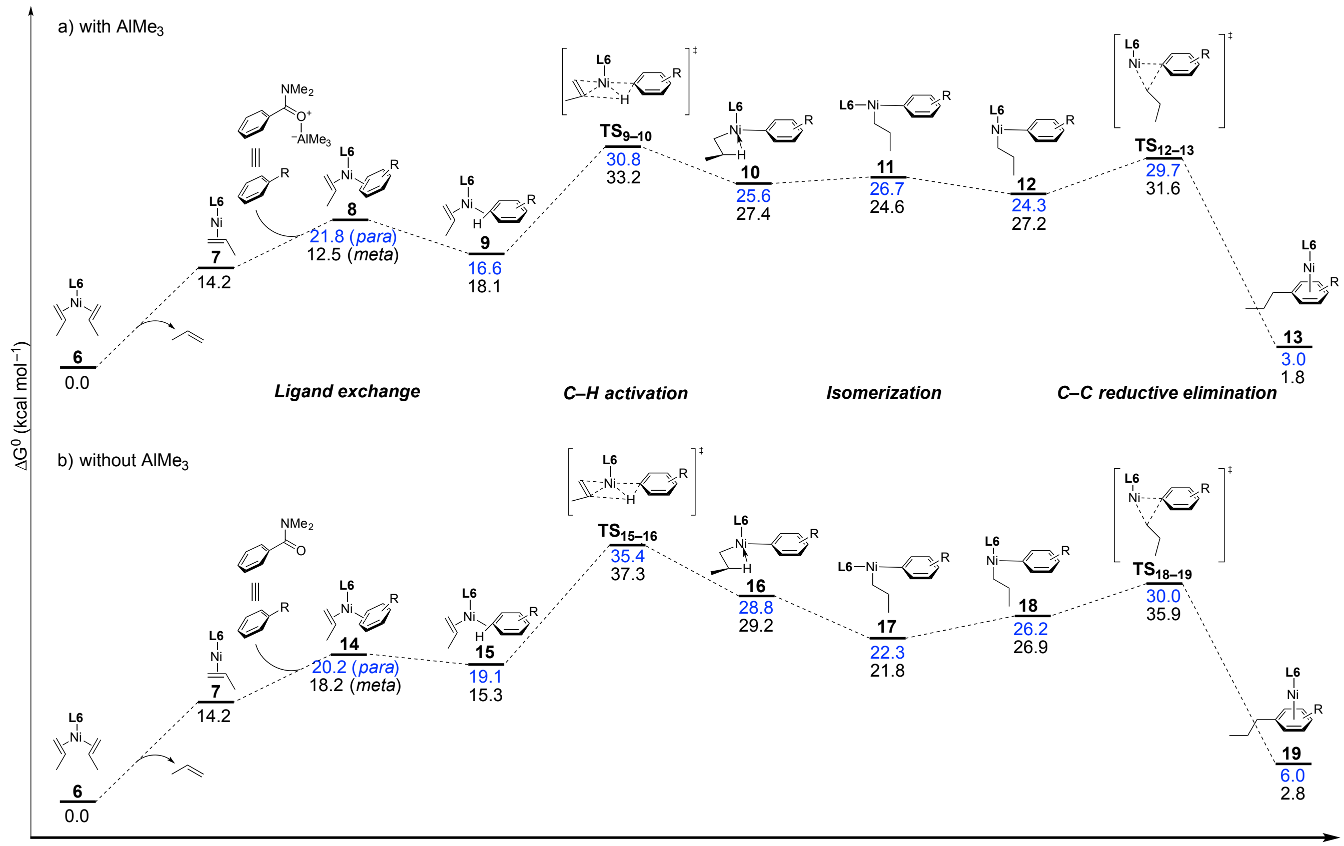

Figure 1. Changes in geometry and Gibbs energy in the alkylation of *N*,*N*-dimethylbenzamide catalyzed by (a) (**L6**)Ni/$AlMe_3$ system and (b) (**L6**)Ni system. Values in blue represent the energy changes in the *para*-alkylation and those in black for the *meta*-alkylation.

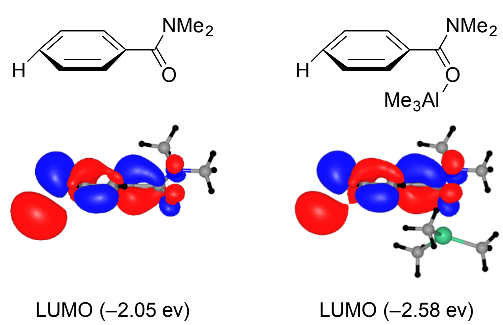

Figure 2. LUMOs of *N*,*N*-dimethylbenzamide and its $AlMe_3$ adduct whose geometries are taken to be the same as in the transition state for C–H σ-bond cleavage

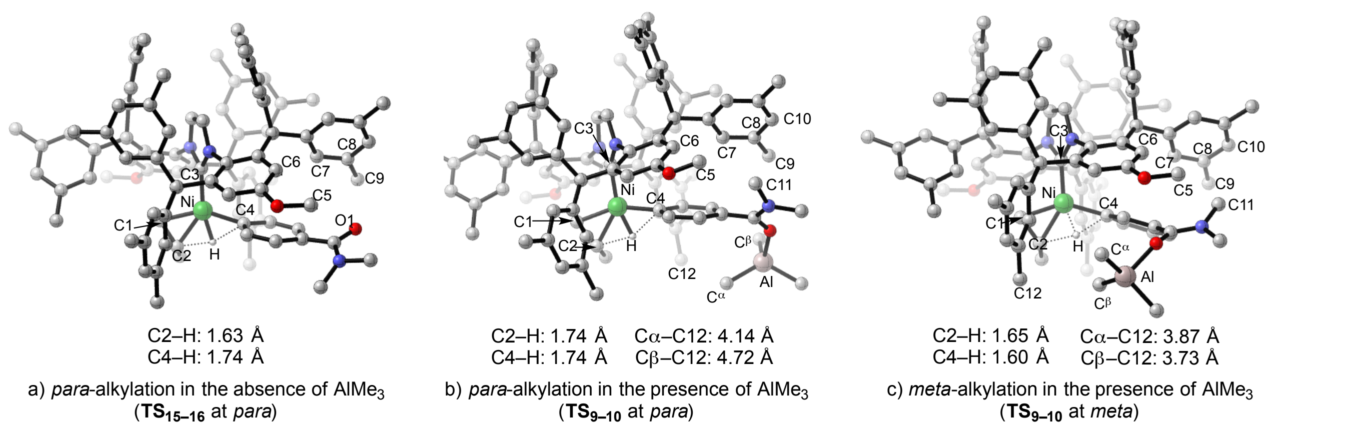

Figure 3. Transition states of the C–H σ-bond cleavage of *N*,*N*-dimethylbenzamide by (**L6**)Ni(propene)

ASSOCIATED CONTENT

Supporting Information. Detailed experimental procedures including spectroscopic and analytical data (PDF). This material is available free of charge via the Internet at http://pubs.acs.org.

AUTHOR INFORMATION

Corresponding Author

sakaki.shigeyoshi.47e@st.kyoto-u.ac.jp
nakao.yoshiaki.8n@kyoto-u.ac.jp

ACKNOWLEDGMENT

This article is dedicated to Professor Tamejiro Hiyama on the occasion of his 70th birthday. This work was supported by the CREST program “Establishment of Molecular Technology towards the Creation of New Functions” Area from JST (Y.N. and S.S.) and by Grant-in-Aids for Young Scientists (A) (25708006 to Y.N.) and Research on Innovative Areas “Precise Formation of a Catalyst Having a Specified Field for Use in Extremely Difficult Substrate Conversion Reactions” (no. 15H05799 to Y.N.) from MEXT.

REFERENCES

(1) Trost, B. M. *Angew. Chem. Int. Ed*. **1995**, *53*, 259.

(2) Perego, C.; Ingallina, P. *Catal. Today* **2002**, *73*, 3.

(3) Gilman, H.; Burtner, R. R. *J. Am. Chem. Soc*. **1935**, *59*, 909.

(4) Kakiuchi, F.; Kochi, T. *Synthesis* **2008**, *19*, 3013.

(5) Murai, S.; Kakiuchi, F.; Sekine, S.; Tanaka, Y.; Kamatani, A.; Sonoda, M.; Chatani, N. *Nature* **1993**, *366*, 529.

(6) Crisenza, G. E. M.; McCreanor, N. G.; Bower, J. F. *J. Am. Chem. Soc*. **2014**, *136*, 10258.

(7) Guo, X.; Li, C.-J. *Org. Lett*. **2011**, *13*, 4977.

(8) Wang, X.; Leow, D.; Yu, J.-Q. *J. Am. Chem. Soc*. **2011**, *133*, 13864.

(9) Yadagiri, D.; Anbarasan, P. *Org. Lett*. **2014**, *16*, 2510.

(10) Yu, D.-G.; de Azambuja, F.; Glorius, F. *Angew. Chem. Int. Ed.* **2014**, *53*, 7710.

(11) Jia, S.; Xing, D.; Zhang, D.; Hu, W. *Angew. Chem. Int. Ed.* **2014**, *53*, 13098.

(12) Yu, Z.; Ma, B.; Chen, M.; Wu, H.-H.; Liu, L.; Zhang, J. *J. Am. Chem. Soc*. **2014**, *136*, 6904.

(13) Cong, X.; Zeng, X. *Org. Lett*. **2014**, *16*, 3716.

(14) Hu, X.; Martin, D.; Melaimi, M.; Bertrand, G. *J. Am. Chem. Soc*. **2014**, *136*, 13594.

(15) Cheng, C.; Hartwig, J. F. *Science* **2014**, *343*, 853.

(16) Saito, Y.; Segawa, Y.; Itami, K. *J. Am. Chem. Soc*. **2015**, *137*, 5193.

(17) Bag, S.; Patra, T.; Modak, A.; Deb, A.; Maity, S.; Dutta, U.; Dey, A.; Kancherla, R.; Maji, A.; Hazra, A.; Bera, M.; Maiti, D. *J. Am. Chem. Soc*. **2015**, *137*, 11888.

(18) Nakao, Y.; Yamada, Y.; Kashihara, N.; Hiyama, T. *J. Am. Chem. Soc*. **2010**, *132*, 13666.

(19) Gómez-Suárez, A.; Ramón, R. S.; Songis, O.; Slawin, A. M. Z.; Cazin, C. S. J.; Nolan, S. P. *Organometallics* **2011**, *30*, 5463.

(20) Meiries, S.; Speck, K.; Cordes, D. B.; Slawin, A. M. Z.; Nolan, S. P. *Organometallics* **2013**, *32*, 330.

(21) Tamao, K.; Ishida, N.; Tanaka, T.; Kumada, M. *Organometallics* **1983**, *2*, 1694.

(22) Hiyama, T. in *Organometallics in Synthesis, Third Manual*; Schlosser, M. Ed.; John Wiley & Sons, 2013; 373.

(23) Martin, R.; Romea, P.; Tey, C.; Urpi, F.; Vilarrasa, J. *Synlett* **1997**, 1414.

(24) Sonoda, M.; Kakiuchi, F.; Kamatani, A.; Chatani, N.; Murai, S. *Chem. Lett*. **1996**, *25*, 109.

(25) Aryl fluorides can be converted via C–F bond activation, that could compensate for the limited functional group tolerance of the present *para*-alkylation protocols. Amii, H.; Uneyama, K. *Chem. Rev*. **2009**, *109*, 2119.

(26) Bair, J. S.; Schramm, Y.; Sergeev, A. G.; Clot, E.; Eisenstein, O.; Hartwig, J. F. *J. Am. Chem. Soc*. **2014**, *136*, 13098.

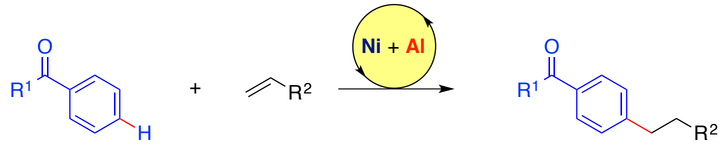

O
R1
H
+
R2
Ni + Al
O
R1
R2